

# Role of Volatility in the Development of JP-8 Surrogates for Diesel Engine Application

Author, co-author (Do NOT enter this information. It will be pulled from participant tab in MyTechZone)

Affiliation (Do NOT enter this information. It will be pulled from participant tab in MyTechZone)

Copyright © 2014 SAE International

## Abstract

Surrogates for JP-8 have been developed in the high temperature gas phase environment of gas turbines. In diesel engines, the fuel is introduced in the liquid phase where volatility plays a major role in the formation of the combustible mixture and autoignition reactions that occur at relatively lower temperatures. In this paper, the role of volatility on the combustion of JP-8 and five different surrogate fuels was investigated in the constant volume combustion chamber of the Ignition Quality Tester (IQT). IQT is used to determine the derived cetane number (DCN) according to ASTM D6890. The surrogate fuels were formulated such that their DCNs matched that of JP-8, but with different volatilities. Tests were conducted to investigate the effect of volatility on the autoignition and combustion characteristics of the surrogates using a detailed analysis of the rate of heat release immediately after the start of injection. In addition, the effect of volatility on the spray dynamics was investigated by Schlieren imaging in an optical accessible rapid compression machine (RCM), and the imaging data supported the conclusion made in the IQT tests. Furthermore, apparent activation energies of JP-8 and surrogate fuels were determined based on the chemical delay periods, which could be considered as a new parameter for developing surrogate fuel.

## Introduction

A better understanding of the autoignition and combustion characteristics of alternative fuels [1-3] in internal combustion (IC) engines is needed, to improve engine performance, emissions, and fuel economy. Gaining this understanding via experimentation is very challenging because real fuels, such as JP-8, are composed of thousands of components for which the combustion mechanisms are not known. A reasonable approach is to develop a surrogate fuel with a defined composition that mimics the characteristics and properties of the real fuel. Generally, the surrogate fuel is supposed to have (i) a limited number of components, (ii) similarity in properties and combustion characteristics to the real fuel, (iii) high purity, and (iv) low cost. Due to the different interests of study, a surrogate fuel can be proposed to emulate certain properties of the real fuel [4]. Surrogate fuels can be typically classified as physical surrogates that match the physical properties of the real fuel, such as distillation curve, density, and viscosity, and chemical surrogates that match the chemical properties of the real fuel, such as soot tendency, ignition delay, species, and etc [5,6].

In the past decades, many proposed surrogate fuels have been studied in different experimental devices [7-20]. A pressurized flow reactor (PFR) is widely used to investigate the Negative Temperature Coefficient (NTC) regime, reactivity and intermediate species during low temperature oxidation of fuels. Lenhart [5], Agosta [6], and Cemansky [8] found that strong NTC behavior was observed for all JP-8 samples. However, none of the surrogate fuels matched the start of the NTC regime with JP-8 samples although some surrogates provided the closest match to the reactivity. Moreover, the study suggested that increasing the overall aromatic content of a fuel would tend to decrease reactivity but cause no significant effects on the start of the NTC region. Dooley et al. reported that their first (n-decane/iso-octane/toluene) and second (n-dodecane/iso-octane/1,3,5-trimethylbenzene/n-propylbenzene) generation surrogate fuels produced a very similar concentration of intermediate species compared to the real fuel during low temperature oxidation processes although the first generation surrogate fuel was much more volatile than the second generation surrogate fuel [9,10]. Based on previous studies, an important corollary is that two fuels should have very similar oxidation characteristics in fundamental experiments if the main combustion property targets are matched, such as derived cetane number (DCN), hydrogen-carbon ratio (H/C), molecular weight (MW), and threshold sooting index (TSI) [9-14].

In order to examine global combustion kinetic behavior, shock tubes and rapid compression machines (RCM) are the most commonly used to obtain ignition delay (ID), pressure and rate of heat release (RHR) traces. Studies have shown that the IDs of surrogate fuels were very close to the actual fuel in a shock tube [9-12,15] although the two-stage ignition from the pressure and RHR traces exhibited a great difference from that of the actual fuel in a RCM [9,10]. Other aspects of surrogate fuels have also been investigated in different types of experimental systems. Honnet [16] reported that the Aachen (n-decane/1,2,4-trimethylbenzene) surrogate fuel accurately reproduces the extinction strain rate and volume fraction of soot formation in laminar non-premixed flows. Humer [17] indicated that the extinction characteristics of Aachen and modified Aachen (n-dodecane/1,2,4-trimethylbenzene) surrogate fuels agree well with JP-8 in laminar non-uniform flows.

It should be noted that most of the surrogate work in PFR, shock tube, and RCM were conducted with fuels in the gas phase. However, few studies have shown differences in

Report Documentation Page				Form Approved OMB No. 0704-0188	
Public reporting burden for the collection of information is estimated to average 1 hour per response, including the time for reviewing instructions, searching existing data sources, gathering and maintaining the data needed, and completing and reviewing the collection of information. Send comments regarding this burden estimate or any other aspect of this collection of information, including suggestions for reducing this burden, to Washington Headquarters Services, Directorate for Information Operations and Reports, 1215 Jefferson Davis Highway, Suite 1204, Arlington VA 22202-4302. Respondents should be aware that notwithstanding any other provision of law, no person shall be subject to a penalty for failing to comply with a collection of information if it does not display a currently valid OMB control number.					
1. REPORT DATE <b>01 MAR 2014</b>		2. REPORT TYPE <b>Journal Article</b>		3. DATES COVERED <b>09-10-2013 to 13-01-2014</b>	
4. TITLE AND SUBTITLE <b>Role of Volatility in the Development of JP-8 Surrogates for Diesel Engine Application</b>				5a. CONTRACT NUMBER	
				5b. GRANT NUMBER	
				5c. PROGRAM ELEMENT NUMBER	
6. AUTHOR(S) <b>Zheng Zheng; Po-I Lee; Naeim Henein</b>				5d. PROJECT NUMBER	
				5e. TASK NUMBER	
				5f. WORK UNIT NUMBER	
7. PERFORMING ORGANIZATION NAME(S) AND ADDRESS(ES) <b>Wayne State University, 42. W. Warren Ave, Detroit, Mi, 48202</b>				8. PERFORMING ORGANIZATION REPORT NUMBER <b>; #24279</b>	
9. SPONSORING/MONITORING AGENCY NAME(S) AND ADDRESS(ES) <b>U.S. Army TARDEC, 6501 East Eleven Mile Rd, Warren, Mi, 48397-5000</b>				10. SPONSOR/MONITOR'S ACRONYM(S) <b>TARDEC</b>	
				11. SPONSOR/MONITOR'S REPORT NUMBER(S) <b>#24279</b>	
12. DISTRIBUTION/AVAILABILITY STATEMENT <b>Approved for public release; distribution unlimited</b>					
13. SUPPLEMENTARY NOTES <b>Submitted to 2014 SAE World Congress</b>					
14. ABSTRACT <b>Surrogates for JP-8 have been developed in the high temperature gas phase environment of gas turbines. In diesel engines, the fuel is introduced in the liquid phase where volatility plays a major role in the formation of the combustible mixture and autoignition reactions that occur at relatively lower temperatures. In this paper, the role of volatility on the combustion of JP-8 and five different surrogate fuels was investigated in the constant volume combustion chamber of the Ignition Quality Tester (IQT). IQT is used to determine the derived cetane number (DCN) according to ASTM D6890. The surrogate fuels were formulated such that their DCNs matched that of JP-8, but with different volatilities. Tests were conducted to investigate the effect of volatility on the autoignition and combustion characteristics of the surrogates using a detailed analysis of the rate of heat release immediately after the start of injection. In addition, the effect of volatility on the spray dynamics was investigated by Schlieren imaging in an optical accessible rapid compression machine (RCM), and the imaging data supported the conclusion made in the IQT tests. Furthermore, apparent activation energies of JP-8 and surrogate fuels were determined based on the chemical delay periods, which could be considered as a new parameter for developing surrogate fuel.</b>					
15. SUBJECT TERMS					
16. SECURITY CLASSIFICATION OF:			17. LIMITATION OF ABSTRACT <b>Public Release</b>	18. NUMBER OF PAGES <b>15</b>	19a. NAME OF RESPONSIBLE PERSON
a. REPORT <b>unclassified</b>	b. ABSTRACT <b>unclassified</b>	c. THIS PAGE <b>unclassified</b>			



thermophysical properties of an actual fuel and its surrogate fuels, such as distillation curve, density, sound speed, viscosity, and thermal conductivity [18-22]. The surrogate fuels proposed by Violi [23] show a better fit of the distillation characteristics to mimic the volatility of JP-8. However, this study did not include experimental work to examine the effect of volatility on autoignition and combustion characteristics. Therefore, there is an interest in investigating the importance of volatility in surrogate development for diesel engine applications in terms of spray, autoignition, and combustion characteristics in multi-phase heterogeneous combustion conditions.

## Experiments

### Optical Accessible Rapid Compression Machine

The RCM is mainly designed to emulate an engine compression stroke to make fundamental analysis of IC engine cycle combustion. Thus, it has the following advantages: (i) easy access of various optical diagnostic techniques, (ii) flexibility and accuracy in controlling the charge pressure and temperature, (iii) easy to clean windows. A detailed description and operating procedure have been provided in previous publications [24-26].

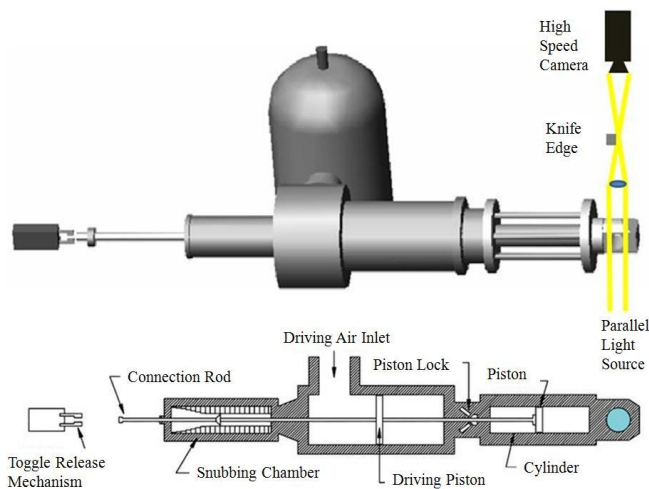


Figure 1. Schematic of rapid compression machine at Wayne State University

A schematic of the RCM is shown in Figure 1. Three pistons with different functions are mounted on a long connection rod and located inside three cylinders or chambers. The first piston on the left is in the snubbing chamber, which is filled with viscous hydraulic oil in the funnel shape chamber and provides the damping resistance of the compression stroke. The second chamber in the middle with pressurized shop air generates the force to perform a compression stroke. In this study, the driving air is set at 60 psi. The charge air contained in the third cylinder is compressed into a combustion chamber through a check valve and orifice when the compression stroke occurs. The charge air is pre-heated and kept at the pressure of 1 bar and temperature of 373 K. Once the charge air is compressed, the peak pressure can reach about 18 bar. In order to avoid turbulence interference during the Schlieren tests, the compressed air has settled down for about 10 seconds after the piston reached its top dead center (TDC). Thus, the corresponding pressure and mass average temperature at the

injection signal are 15 bar and 600 K, respectively. A sample pressure history, with injection and camera signals, is shown in Figure 2.

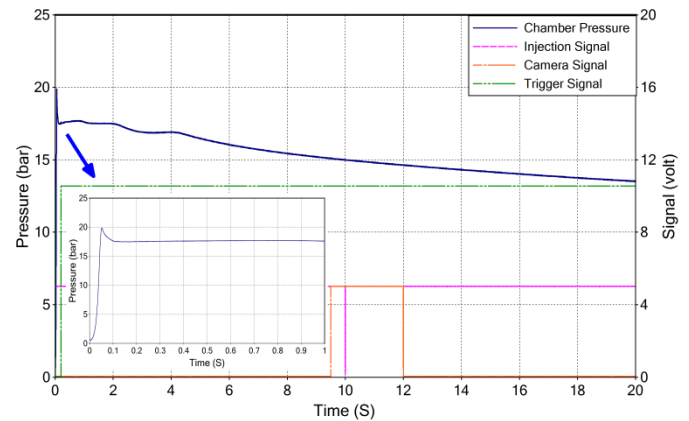


Figure 2. Sample signal traces of a rapid compression machine

The fuel sprays were studied in an optical accessible combustion chamber of the RCM under simulated, quiescent diesel engine conditions. A schematic of the Schlieren visualization setup along with the chamber is shown in Figure 3. The chamber is in a cylindrical shape with two quartz windows on both side ports, which allow line-of-sight imaging of the injected fuel spray. A common rail solenoid injector with a single-hole nozzle is mounted at an angle about  $28^\circ$  from the vertical axis, delivering the fuel into the center of the combustion chamber at the injection pressure of 100 bar. Due to the size of the chamber, the injection duration was well controlled to be same for all the fuels and to avoid serious impingement on the walls and windows. This non-ignitable condition was selected intentionally to isolate the mixing and evaporation processes from the complex autoignition and combustion processes. In addition, a Kistler type 6117B spark plug with an integrated pressure transducer is installed on the horizontal axis.

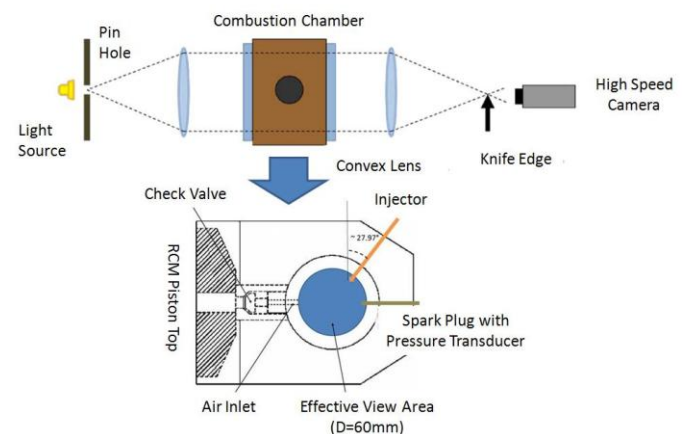


Figure 3. Schematic visualization setup for the combustion chamber of a rapid compression machine

A 70W projection lamp provided light source passing through a small pin hole, which was placed on the focal point of a convex lens. Thus, the point light source was converted to parallel light, which proceeded through the chamber where injection events take place, and reached another convex lens. A sharp

knife edge was placed on the focal point of second lens to cut the refracted light beam, which was refocused to a high-speed CMOS camera (Vision Research Phantom V310). Images were collected at approximate 10000 frame per second (FPS) and with 512 by 512 pixel resolutions. A detailed Schlieren setup has been provided in previous publications [27-29].

## Ignition Quality Tester

The Ignition Quality Tester (IQT) [30] is widely used to measure the DCN of fuels for diesel engines. Also, DCN is considered as one of the critical properties in the investigation of surrogates for aviation fuels [9-10,13]. A detailed description of IQT at Wayne State University, as well as details of its operation, have been provided in previous investigations [31,32].

As in the IQT study, a fuel was injected into the combustion chamber along the central axis of the body, which is pre-heated to the standard test temperature of about 828 K by nine cartridge-type resistance heaters. The charge air pressure and temperature are  $2.137 \pm 0.007$  MPa and  $818 \pm 30$  K, respectively [30]. The IQT is a high temperature combustion device that simulates compression temperatures in diesel engines but at a lower air pressure.

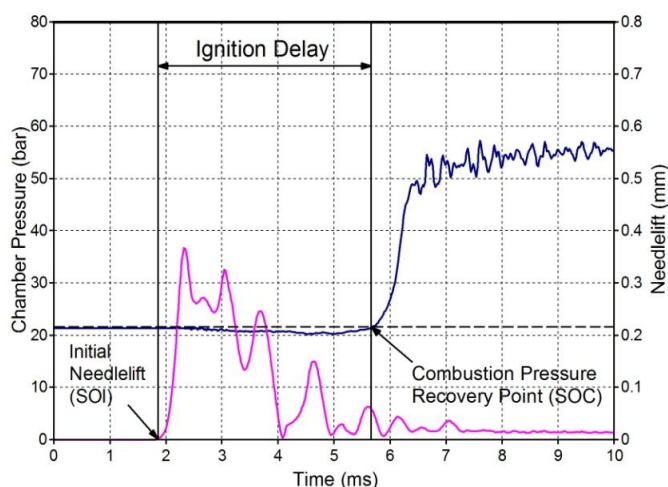


Figure 4. A sample of traces for the needlelift and chamber pressure depicting the definition of IQT ignition delay time

The IQT equipment was utilized in the present investigation as a platform to investigate the physical and chemical processes that lead to the autoignition of different fuels under well-controlled charge pressure and different temperatures. There are many definitions of the ignition delay period in the literature. All researchers agree on the start of injection (SOI) as the start of ID. However, several criteria have been used to define the end of ID or the start of combustion (SOC) [33-36]. In the current investigation, the definition of ID specified in ASTM D6890 [30] was used as shown in Figure 4. It is the time elapsed from the SOI to the SOC. SOC in ASTM D6890 is defined as the time when the pressure in the chamber reaches 138 kPa above the initial chamber pressure. This point is considered to be the "combustion recovery point" [37-38].

A schematic of IQT is shown in Figure 5. There are two thermocouples inside the combustion chamber along the axial direction. The first thermocouple measures the charge

temperature close by the injector nozzle, and the second thermocouple is 7 cm downstream from the first one. The temperature gradient increases approximately 30 K from the first to the second thermocouple [38,39]. The local area where combustion starts in the IQT is close to the pressure transducer [38]. In order to capture the change in temperature during the autoignition process, the thermocouple at position "a" was replaced with an Omega K-type fast response 0.002" diameter junction. The thermocouple is connected to a compensation circuit with an amplifier module (Analog Device 5B40).

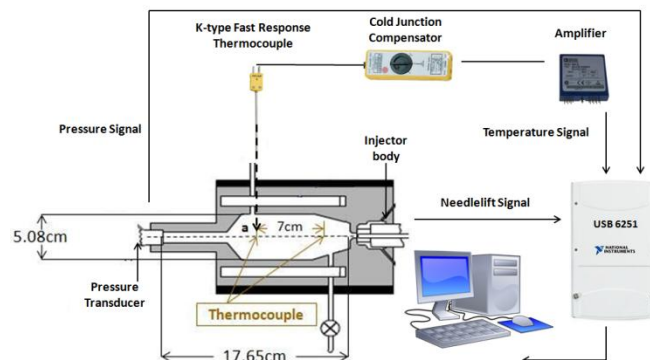


Figure 5. Schematic of IQT with a fast-response thermocouple and the additional DAQ system (based on reference [38])

An additional National Instrument (NI) high-speed multifunction data acquisition (DAQ) system was connected to the standard IQT system to expand the capability of obtaining data. The needlelift (N.L), pressure and temperature signals were simultaneously measured at a sampling rate of 1.25 MS/s. All the safety features were controlled by the standard IQT system.

## Fuels

### Volatility

Unlike conventional diesel fuel, JP-8 is not well classified and has a wide range of cetane numbers (CN) and volatility. The overall volatility of a fuel can be identified by its distillation curve [23]. In the current investigation, the distillation curve of a specific lot of JP-8 fuel was measured at the Southwest Research Institute (SwRI) according to ASTM D86 [40], the other properties of JP-8 are shown in the Appendix. The distillation curves of the surrogate fuels were calculated using the Aspen HYSYS [41] software package, and the Peng-Robinson model was chosen to solve the state equations, based on ASTM D86.

### Derived Cetane Number

In previous publications of surrogate development, the DCN of a surrogate fuel was calculated based on a linearity assumption between the volume fraction and the DCN of its components [20, 42]. However, calculated DCNs are not always consistent with measured DCNs [42]. Thus, the DCNs of all the surrogate fuels in the current study were measured in IQT. The choice of the surrogate components was guided by data published in the literature. In order to compare the effects of volatility on autoignition and combustion characteristics, some minor modifications were made to their volume



percentages to keep the same DCNs of surrogate fuels. Meanwhile, other properties such as density, H/C, MW of the surrogate fuels were optimized to match the target JP-8 by using a MATLAB code. The detailed description was provided in a previous publication [42].

### Density

In a multi-phase heterogeneous combustion system, density is a very important factor for autoignition processes because a fuel is injected by volume in diesel engines. Also, the same density of a fuel implies the same mass of fuel injected into the combustion chamber, which is related to the global equivalence ratio and heating value. Thus, the density of surrogate fuels was optimized to match the target JP-8.

### Low Heating Value

Low heating value (LHV) is the amount of energy released during combustion of the specified amount of a fuel, and it is very important to diesel engine applications. Thus, the LHVs of surrogate fuels were optimized to match the target JP-8.

### Hydrogen-Carbon Ratio

H/C ratio is closely related to the adiabatic flame temperature, local air-fuel stoichiometry, enthalpy of autoignition reactions, flame speed, etc [43]. Thus, the H/C ratios of surrogate fuels were optimized to match the target JP-8.

Table 1. Properties of JP-8 and surrogate fuels with their composition

Fuel	JP-8	SF1	SF2	SF3	SF4	SF5
n-C16	-	-	-	-	-	1
n-C12	-	-	-	60	36	49
n-C10	-	54	66	-	14	-
i-C16	-	-	-	-	24	16
i-C8	-	30	-	-	-	-
decalin	-	-	-	-	-	19
MCH	-	-	-	-	8	-
TMB	-	-	34	40	-	11
xylene	-	-	-	-	-	4
toluene	-	16	-	-	18	-
DCN	49.24*	49.51*	49.1*	49.28*	49.4*	49.28*
Density (g/ml)	0.802*	0.74	0.78	0.802	0.774	0.805
LHV (MJ/kg)	43.2*	44.1	43.4	43.2	44.1	43.7
H/C	1.93*	2	1.86	1.79	1.98	1.93
MW (g/mol)	161*	122	133	144	142	157
TSI	22.96*	14.6	28.94	35.27	16.32	22.19

\*measured

### Other Properties of Surrogates

The average MW is correlated with fuel diffusion processes in the gas phase [44]. Threshold Sooting Index (TSI) is an overall measure of the tendency for soot formation. Thus, these

properties of surrogate fuels were optimized to be close to the target JP-8 although the correlation between TSI and particulate matter formation in diesel engines is not known at the present time.

The following six fuels were tested in the current study: (i) JP-8, a military aviation fuel; (ii) surrogate fuel #1 [9], denoted as "SF1"; (iii) surrogate fuel #2 [16,17,45], denoted as "SF2"; (iv) surrogate fuel #3 [17], denoted as "SF3"; (v) surrogate fuel #4 [46], denoted as "SF4"; and (vi) surrogate fuel #5 [5,23], denoted as "SF5". It should be noted that the selection of pure components was guided by the previous publications and the minor modification were made to match the properties of current JP-8 batch at Wayne State University (WSU). The properties and composition (volume basis) of tested fuels are listed in Table 1. The pure components used in this study are as follows: (a) n-hexadecane, as "n-C16", (b) n-dodecane, as "n-C12", (c) n-decane, as "n-C10", (d) 2,2,4,4,6,8,8-heptamethylnonane (iso-cetane), as "i-C16", (e) 2,2,4-trimethylpentane (iso-octane), as "i-C8", (f) decahydronaphthalene, as "decalin", (g) methylcyclohexane, as "MCH", (h) 1,2,4-trimethylbenzene, as "TMB", (i) m-xylene, as "xylene", and (j) toluene. The detailed pure component information is shown in the Appendix.

## Results and Discussion

### Distillation curves of the surrogates and JP-8

Prior to simulating the distillation curves for the surrogate fuels developed in this investigation, the accuracy of Aspen HYSYS software predictions were compared with distillation curves developed experimentally at SwRI. Figure 6 shows a fairly good agreement between the predicted and measured data for SF1, SF2, and SF3.

The distillation curves calculated using Aspen HYSYS software for the five surrogate fuels of Table 1 are shown in Figure 7, along with the curve measured for JP-8.

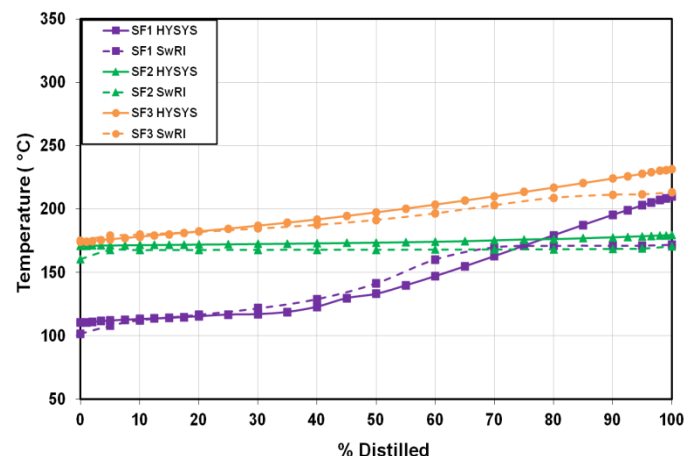


Figure 6. Comparison of distillation curves developed using HYSYS simulation and SwRI experimental results for three surrogate fuels.

SF1 is the most volatile surrogate fuel followed by SF4. The high volatility of SF1 is related to high volatility of its

components, such as 2,2,4-trimethylpentane and toluene, which affects the volatility particularly at low temperatures. It is worth noting that low temperature evaporation is very critical to diesel engine performance [47]. The SF2 shows almost a straight line due to the close boiling points of 1,2,4-trimethylbenzene (169 °C) and n-decane (174 °C) [48]. SF3 shows a very close trend to JP-8 with a difference of about 10 °C. With an increasing number of surrogate components, a better fit of the distillation curve was achieved such as with SF5 which matches the JP-8 curve from the initial to final boiling points.

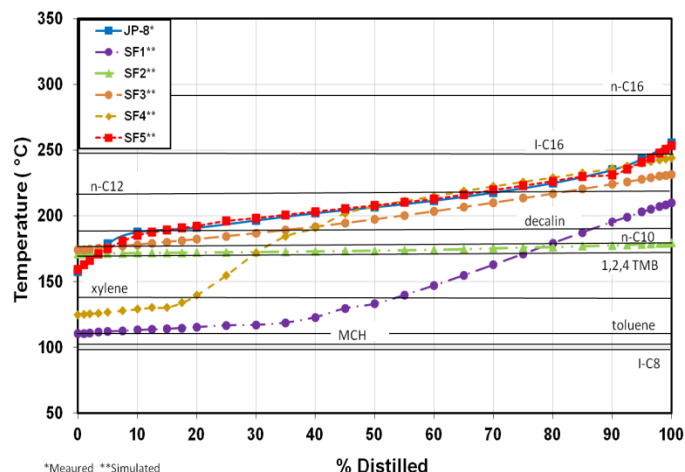


Figure 7. Comparison of distillation curves between JP-8 and surrogate fuels

### Optically Accessible Rapid Compression Machine

The effects of volatility on the spray characteristics of each surrogate fuel and JP-8 were examined in the RCM at a charge pressure of 15 bar and a temperature of 600 K. The SOI was determined in the images by one frame prior to the first appearance of the initial jet. The high-speed Schlieren images were processed to obtain the spray penetration and projected vapor area. The raw Schlieren images showed a dark vaporized jet over a bright background, which is difficult to analyze because the background is not uniformly bright between each test. Further, it is quite challenging to define the vapor boundary just based on raw images. Thus, in the current study, a MATLAB based image processing code has been developed for this analysis [29]. A raw image was subtracted from a background image to reduce the effect of inhomogeneity of the light source, which also eliminated black spots caused by dust on the windows and the lens. In addition, a threshold (7% of maximum intensity) was applied for boundary calculation. In this study, spray penetration was defined as the length from the nozzle tip to the tip of the spray plumes, which indicates how far the spray travels with respect to time. Further, the averaged penetrations of each fuel are compared in the results section.

Figure 8 shows raw images with dark spray and bright background, background-subtracted images with gray scale spray and dark background, and binary images with white spray and black background for JP-8 and its surrogate fuels at each corresponding time. The projected areas of each fuel are clearly visible, and the boundaries of fuel vapor are in red. In addition, the liquid region appears darker in the Schlieren

images. At the early stage of injection events, most of the vapor accumulates at the sides of the spray until 0.7 ms after SOI because air entrainment occurs in spray envelopes. Due to the expanding vapor cloud and mixing by more air entrainment, spray shapes are changed gradually and distinguished among different fuels. For instance, the SF1 is observed to have more plumes than the SF5 at 1.7 ms after SOI, compared to JP-8, and it is evident that the SF1 has the largest projected area and the shortest vapor penetration in the images. On the contrary, the SF3 and SF5 exhibit vapor penetration and projected areas similar to that of JP-8.

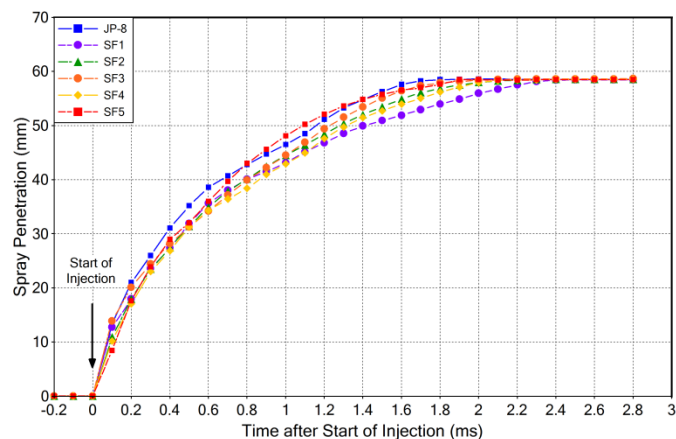


Figure 9. Comparison of vapor penetrations between JP-8 and surrogate fuels

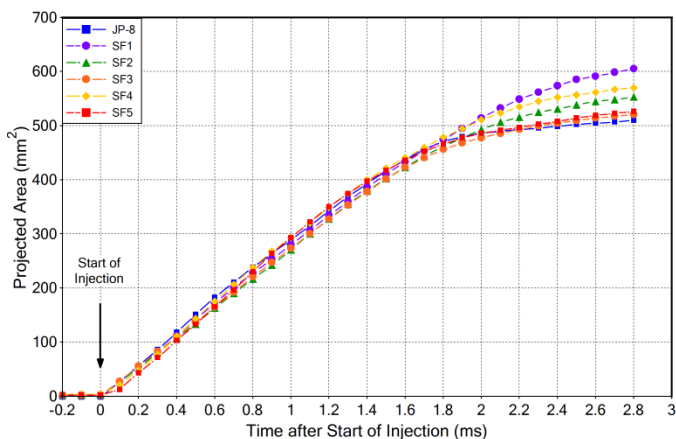


Figure 10. Comparison of projected areas between JP-8 and surrogate fuels

The comparison of vapor penetrations and projected areas among fuels is shown in Figures 9 and 10, which show the results averaged from 5 tests for each fuel. It is observed that spray penetrations were identical for all fuels up to about 0.7 ms. After that, the SF1 started to slow down on the penetration but increased in the projected area. On the other hand, the penetrations of the SF3 and SF5 traveled ahead with relatively small projected areas, and their spray characteristics were close to that of JP-8 during the same time frame, as shown in Figure 8. In addition, the SF4 and SF2 produced slightly longer penetrations than the SF1, but there was no significant difference between them, and the projected area of the SF4 is less than the SF1, but more than the SF2. It can be concluded that the SF1 is the most volatile followed by the SF4 and SF2.

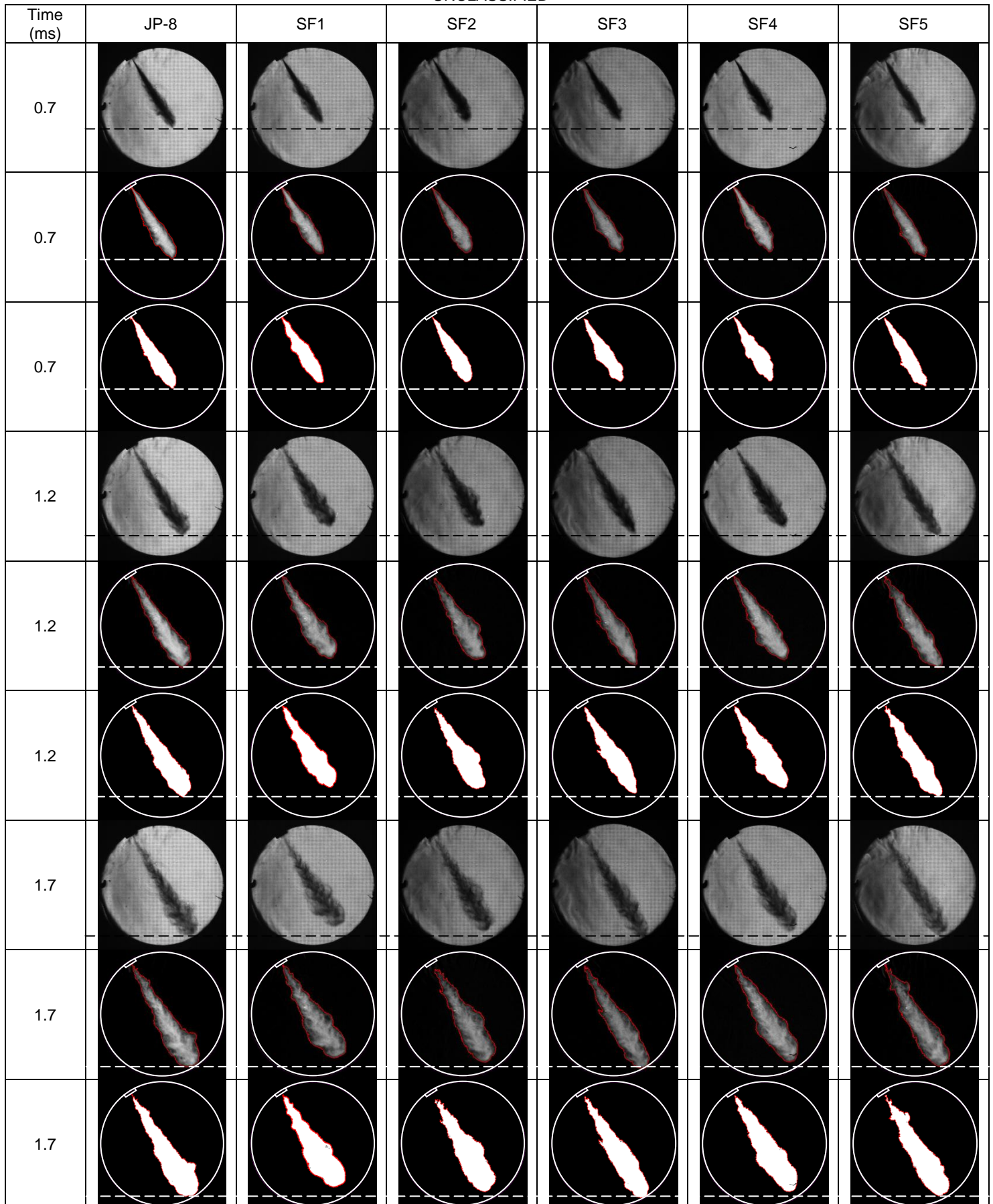




Figure 8. Comparison of raw, background-subtracted, and binary images between JP-8 and surrogate fuels

Conversely, the SF3 and SF5 reveal a similar volatility to that of JP-8. Furthermore, the results of the Schlieren images are consistent with the distillation curves of the fuels. In addition, the unavoidable injection-to-injection variations in the analysis can add potential error into the data.

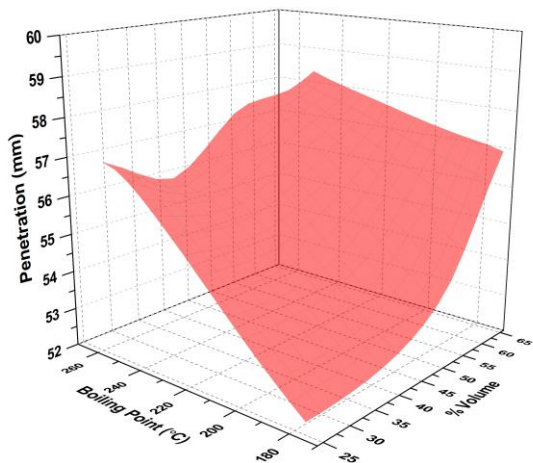


Figure 11. 3D plot of spray penetration, boiling point and volume fraction of pure components

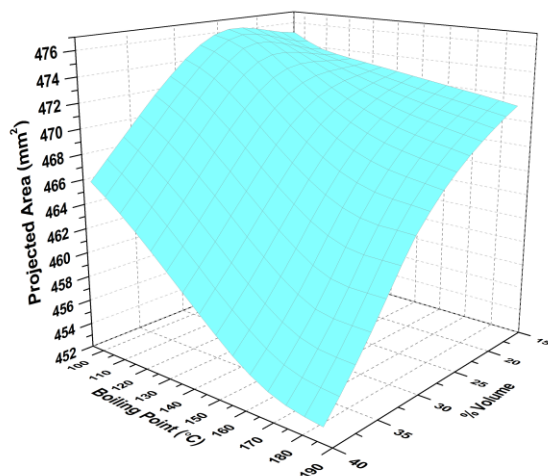


Figure 12. 3D plot of projected area, boiling point and volume fraction of pure components

Figures 11 and 12 are 3D plots of spray penetration and projected area against boiling point of pure components at different volume fractions. It is noticed that vapor penetration increases with increasing the volume percentage of high boiling point components into the surrogate fuel. On the contrary, projected area increases with increasing the volume percentage of low boiling point pure compounds into the surrogate fuel. It should be noted that it is not a linear relationship between the volume fraction of components with different boiling point and spray penetration or projected area, due to the interaction effect of vapor pressure on boiling point between each pure compound according to Raoult's Law [49].

Page 7 of 15

The findings of the vapor penetration and projected areas of different surrogate fuels are important to diesel engine applications since jet-jet interaction, wall impingement and wetting issues need to be considered for different volatility surrogate fuels in engine cylinders.

## Ignition Quality Tester

### Effect of volatility on evaporation processes

In order to investigate the effect of volatility on changes in local temperature during evaporation processes, the surrogate fuels and JP-8 were injected into a nitrogen charge where the autoignition reactions are absent, except for the endothermic fuel dissociation processes. It should be noted that the drop in the pressure, RHR and temperature traces due to endothermic dissociation reactions has been reported to be insignificant if compared with the drop due to the vaporization in the IQT [31].

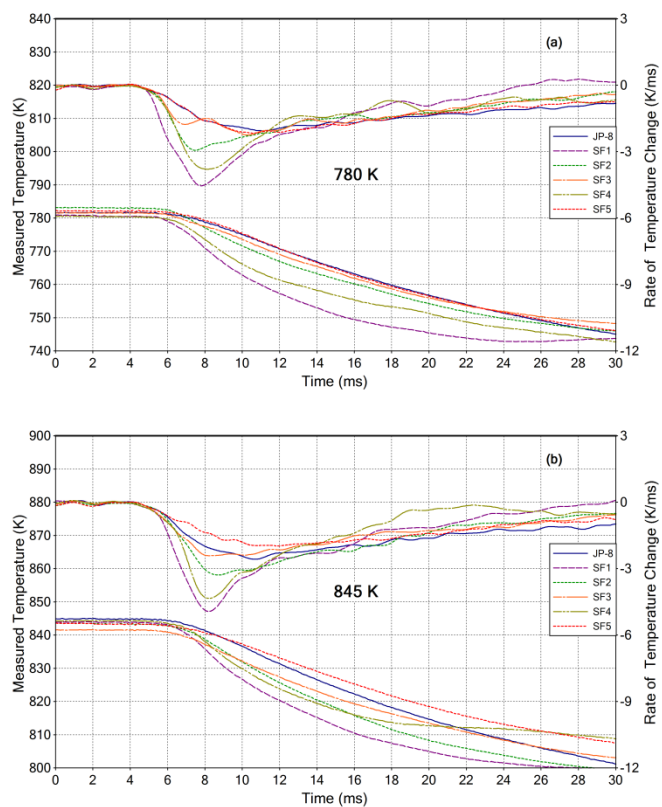


Figure 13a &amp; b. Comparison of temperature profiles between JP-8 and surrogate fuels at 780 and 845 K

Figure 13 shows the measured temperature profiles for JP-8 and surrogate fuels injected into nitrogen. These temperatures were measured by the local thermocouple as shown in Figure 5. It can be observed that the SF1 shows the greatest decrease in temperature profile at both 780 and 845 K due to its high vaporization rate, resulting in more heat absorption at a certain time. In contrast, the temperatures of the SF3 and SF5 were reduced less and exhibit traces similar to that of JP-8, indicating lower volatility than other surrogate fuels. Furthermore, the SF4 shows a higher temperature than the

SF1 but lower than that of the SF2 at 780 K. It also shows a close trend of the SF2 and SF4 at 845 K. It should be noted that autoignition takes place locally, and temperature is directly proportional to the logarithm function of ID. Therefore, the volatility of a surrogate fuel is very important during evaporation processes since autoignition reactions are sensitive to the local temperature.

### Effect of volatility on autoignition and combustion characteristics

The time histories of the gas pressure, needlelift (N.L), and RHR traces are shown in Figure 14 for JP-8 and surrogate fuels at different test temperatures. In this analysis, JP-8 is considered the baseline fuel for comparison with the other surrogate fuels. The figure shows that, for all the fuels, SOI occurs at 1.8 ms and the main injection process is completed in about 2 ms before the rise in pressure due to autoignition. As expected, all the surrogate fuels produced the similar IDs to that of JP-8 because the DCNs were kept as same. However, the SF1 produced a significantly higher peak of RHR, as did the SF4, when compared with JP-8. This is due to these two surrogate fuels containing low boiling point components such as 2,2,4-trimethylpentane (98.5°C), toluene (110.5°C), and methylcyclohexane (101 °C), which affect the overall volatility of a fuel. Moreover, high volatility enhances fuel evaporation and the formation of homogeneity mixture [50], resulting in a sharp rise and higher peak of pressure. The SF2 produced slightly higher peaks of pressure and RHR, indicating that it is more volatile than JP-8. It should be noted that the SF2 has a higher boiling temperature than the SF4 before 30% distillate volume (T50), it still produced a higher peak of RHR than the SF2. This indicates that the low boiling point component of a surrogate fuel is very important for autoignition and combustion characteristics, particularly during the low temperature evaporation and combustible mixture preparation period. Moreover, T50 is not a suitable parameter of volatility considered in the development of surrogate for diesel engine applications. Furthermore, the SF3 and SF5 agree the pressure and RHR traces very well to JP-8, indicating that their volatility is similar to that of the baseline fuel. In addition, the results obtained from pressure and RHR traces show the same volatility trend of each surrogate fuel as in previous sections.

Figure 15 shows the normalized RHR integral for different fuels, from the start of injection to the end of combustion along with the premixed combustion fraction. The SF1 has the highest premixed combustion fraction of 76.5% among all the fuels, while the SF5 has the lowest fraction of 69.5%, which is very close to that of JP-8. Therefore, the findings of autoignition and combustion characteristics for different surrogate fuels are very critical in diesel engines since the premixed combustion fraction, the peak of pressure and RHR, resulting in noise and roughness issues, need to be considered for the development of a surrogate.

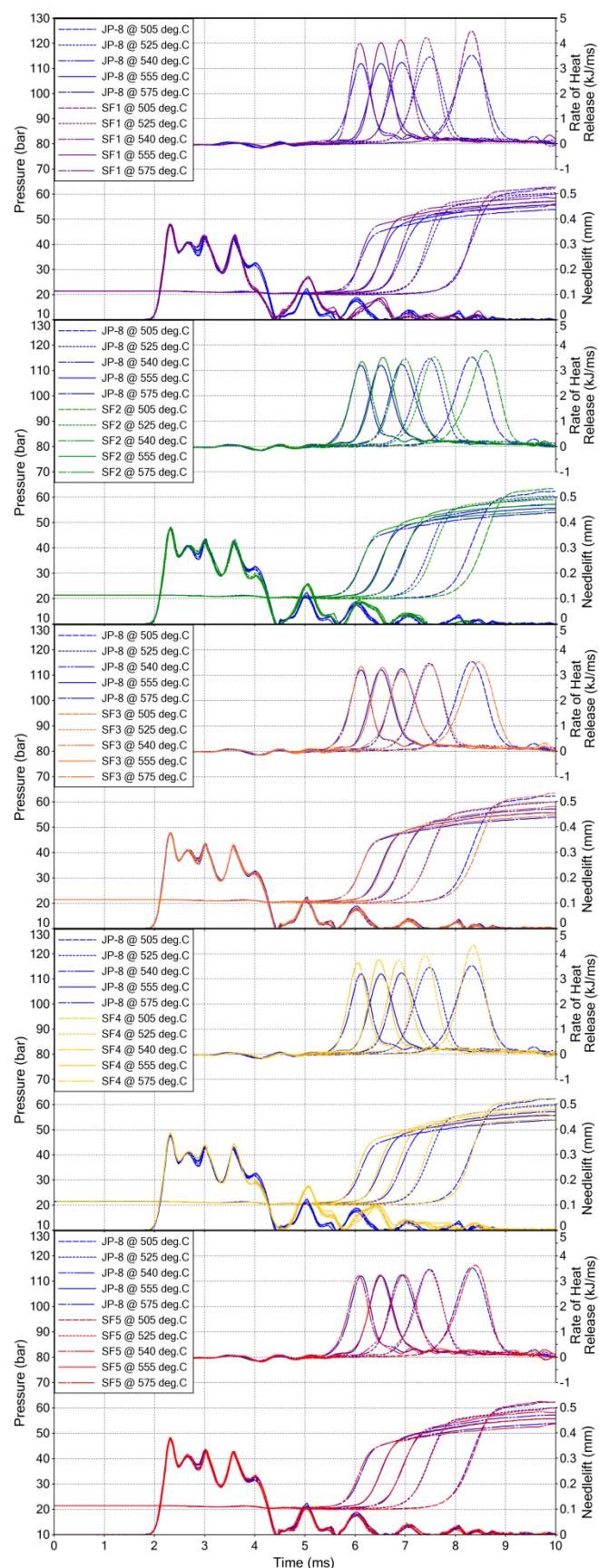


Figure 14. Comparison of pressure, needlelift and RHR traces between JP-8 and surrogate fuels at different temperatures

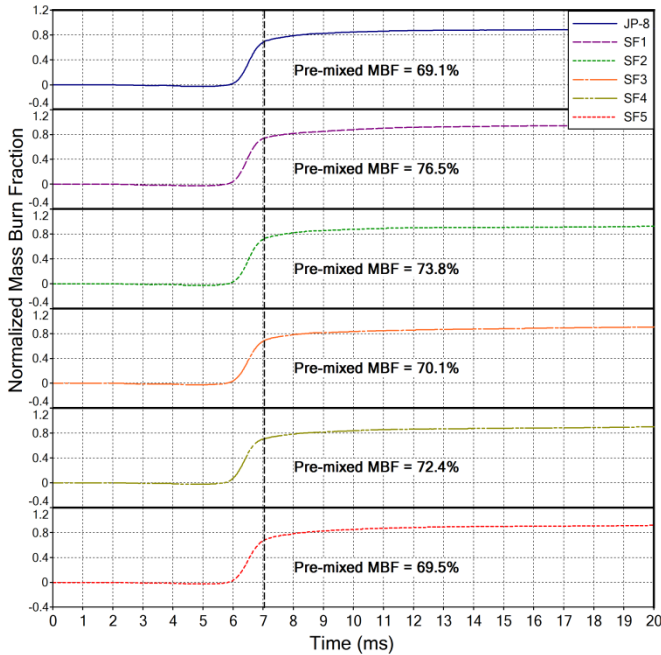


Figure 15. Normalized integral RHR between JP-8 and surrogate fuels

### Arrhenius plot and apparent activation energy

The apparent activation energy is determined based on chemical delay period. In order to separate the physical and chemical delay periods, the fuel was injected into the air and nitrogen charges, respectively, as shown in Figure 16. The trace for injection in nitrogen continues to drop, indicating a continuation of liquid evaporation and endothermic reactions. The trace for injection in air changes its slope, indicating the start of active exothermic reactions. It should be noted that chemical reactions start immediately after fuel is injected. However, the rate of exothermic reactions is so slow that it could not cause a detectable deviation in the pressure and RHR traces, from that with nitrogen. The point of separation between the two traces is defined as the point of inflection (POI), which determines the start of active exothermic reactions or the end of the physical delay period. Therefore, the physical delay is defined as the period of time from SOI to POI, and the chemical delay is defined as the period of time from POI to SOC as shown in Figure 16.

A series of tests were conducted at different charge temperature between 778 and 848 K by controlling the chamber skin temperature. All the tests were conducted at a constant charge pressure of  $21.37 \pm 0.07$  bar ( $310 \pm 1$  psi). The traces were analyzed, and the chemical delays were determined for JP-8 and surrogate fuels at different charge temperatures, as shown in Table 2.

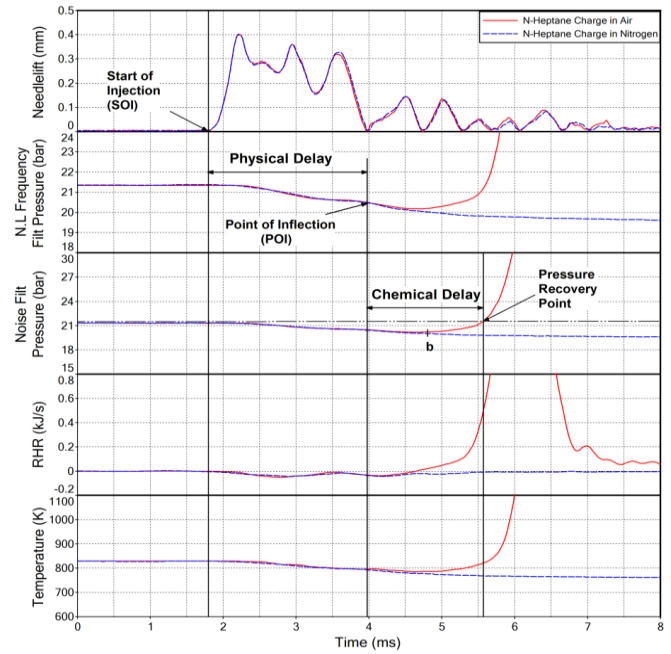


Figure 16. Needlelift, pressure, RHR and temperature traces for fuel injection into air and nitrogen [31]

Table 2. Chemical ignition delays for JP-8 and surrogate fuels at different charge temperatures

Chemical Ignition Delay (ms)						
T (K)	JP-8	SF1	SF2	SF3	SF4	SF5
778	2.34	2.34	2.6	2.42	2.44	2.34
798	2.02	2.02	2.3	2.14	2.1	2.02
813	1.82	1.8	2.08	1.94	1.9	1.8
828	1.7	1.68	1.88	1.82	1.74	1.68
848	1.58	1.56	1.74	1.64	1.6	1.56

The Arrhenius plot is developed of the natural logarithm chemical ID versus the reciprocal of the absolute integrated mean temperature (in Kelvin) during the chemical ID period. The apparent activation energies can be determined from Eqn. 1.

$$\ln\left(\frac{1}{ID}\right) = \ln A - \frac{1000E_a}{R_u T} \quad (1)$$

It should be noted that the activation energies calculated based on Figure 17 do not represent elementary chemical reactions but a large number of known, unknown, simple and complex chemical reactions that occur during the autoignition process [51]. The apparent activation energies,  $E_a$ , of different fuels calculated based on Figure 17 are shown in Table 3.



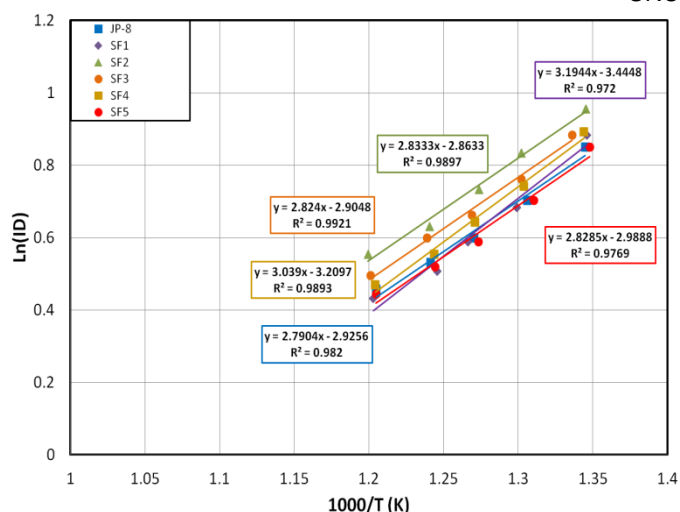


Figure 17. Arrhenius plot based on chemical ignition delay versus mean temperature for JP-8 and surrogate fuels

Table 3 shows that JP-8 has activation energy of 23.19 kJ/mole. Meanwhile, the SF2, SF3 and SF5 have activation energies close to that of JP-8. On the contrary, the SF1 has the highest activation energy of 26.54 kJ/mole, followed by the SF4, with activation energy of 25.25 kJ/mole. The possible reason is that high activation energy components were added to the surrogates such as 2,2,4-trimethylpentane (141 kJ/mole) [52] and toluene (243.1 kJ/mole) [53]. It should be noted that a fuel with a higher activation energy is more sensitive to the change in temperature.

Table 3. Apparent activation energy based on the chemical delay period for JP-8 and surrogate fuels

Fuel	Apparent Activation Energy Ea (kJ/mol)
JP-8	23.19
SF1	26.54
SF2	23.54
SF3	23.47
SF4	25.25
SF5	23.50

The findings of the apparent activation energy of different surrogate fuels are important in diesel engine applications since the same CN fuels do not always produce the same ID in different engine operating conditions; however, the activation energy can be correlated with CN [54,55]. Therefore, activation energy could be considered as a parameter of surrogate development for diesel engine applications.

## Conclusions

The role of volatility in the development of a JP-8 surrogate for diesel engine application was investigated in IQT and optically accessible RCM. Five different surrogate fuels were tested to understand the effect of volatility on spray penetration,

projected area, the drop in local charge temperature due to spray evaporation, RHR, and activation energy for the global autoignition reactions. Meanwhile, several properties of surrogates, such as DCN, density, LHV, H/C, MW, and TSI, were kept close to the target JP-8 to highlight the volatility effects. The following conclusions can be made based on the current investigations:

1. The predicted distillation curves from Aspen HYSYS software agree very well with the experimental data. This software is recommended for use in the development of surrogate for diesel engine application.
2. The higher volatility surrogate fuel shows a shorter spray penetration and a larger projected area than the lower volatility surrogate fuel.
3. The local temperature of the higher volatility surrogate fuel drops at a faster rate due to a higher vaporization rate. The rate of the autoignition reactions is very sensitive to the local charge temperature.
4. The more volatile surrogate fuel produces a higher premixed combustion fraction which results in higher peak of RHR compared to other surrogate fuels.
5. Temperature at 50% distillate volume (T50) is not the best indicator of the volatility of surrogate fuels for diesel engine applications.
6. The boiling point of a pure component affects the spray penetration and projected area of a surrogate fuel, as well as autoignition and combustion characteristics, particularly during the low temperature evaporation and combustible mixture preparation period.
7. The apparent activation energy of the global autoignition reactions could be considered as an additional parameter of surrogate development for diesel engine applications.

Disclaimer: Reference herein to any specific commercial company, product, process, or service by trade name, trademark, manufacturer, or otherwise, does not necessarily constitute or imply its endorsement, recommendation, or favoring by the United States Government or the Department of the Army (DoA). The opinions of the authors expressed herein do not necessarily state or reflect those of the United States Government or the DoA, and shall not be used for advertising or product endorsement purposes.

## References

1. Frame, E. A., Alvarez, R. A., Blanks, M. G., Freerks, R. L., Stavinoha, L., Muzzell, P. A., Villahermosa, L., "Alternative Fuels: Assessment of Fischer-Tropsch Fuel for Military Use in 6.5L Diesel Engine". SAE Technical Paper 2004-01-2961, 2004. DOI: **10.4271/2004-01-2961**.
2. Schihl, P., Hoogterp, L., Pangilinan, H., "Assessment of JP-8 and DF-2 Evaporation Rate of Cetane Number Differences on a Military Diesel Engine". SAE Technical Paper. **2006-01-1549**, 2006. DOI: **10.4271/2006-01-1549**.
3. Schihl, P., Hoogterp, L., Gingrich, E., "The Ignition Behavior of a Coal to Liquid Fischer-Tropsch Jet Fuel in a Military Relevant Single Cylinder Diesel Engine". SAE Technical Paper. **2012-01-1197**, 2012. DOI: **10.4271/2012-01-1197**.

4. Edwards. T., Maurice. L.Q., "Surrogate Mixtures to Represent Complex Aviation and Rocket Fuels", *Journal of Propulsion and Power*, **17**(2): **461-466**, 2001. DOI: **10.2514/2.5765**.
5. Lenhart. D., "The Oxidation of JP-8 and its Surrogates in the Low and Intermediate Temperature Regime", PH.D dissertation, Drexel University, Philadelphia, 2004.
6. Agosta. A., "Development of a Chemical Surrogate for JP-8 Aviation Fuel in Pressurized Flow Reactor", Master thesis, Drexel University, Philadelphia, 2002.
7. Dagaut. T., Cathonnet. M., "The Ignition, Oxidation and Combustion of Kerosene: A review of Experimental and Kinetic Modeling", *Progress in Energy and Combustion Science*, **32**(1): **48-92**, 2006. DOI: **dx.doi.org/10.1016/j.peccs.2005.10.003**.
8. Cemansky, N. P., Miller, D. L., "The Low Temperature Oxidation Chemistry of JP-8 and its Surrogates at High Pressure", Final progress report, DAAD19-03-1-0070, 2006.
9. Dooley, S., Won, S.H., Chaos, M., Heyne, J., Ju, Y., Dryer, F.L., Kumar, K., Sung, C-J., Wang, H., Oehlschlaeger, M.A., Santoro, R.J., and Litzinger, T.A., "A Jet Fuel Surrogate Formulated by Real Fuel Properties", *Combustion and Flame*, **157**, 12, **2333-2339**, 2010.
10. Dooley, S., Won, S., Heyne, J., Farouka, T., Ju, Y., Dryer, F.L., Kumar, K., Hui, X., Sung, C., Wang, H., Oehlschlaeger, M.A., Iyer, V., Iyer, S., Litzinger, T.A., Santoro, R.J., Malwicki, T., Brezinsky, K., "The Experimental Evaluation of a Methodology for Surrogate Fuel Formulation to Emulate Gas Phase Combustion Kinetic Phenomena", *Combustion and Flame*, **159**(4): **1444-1466**, 2012. DOI: **10.1016/j.combustflame.2011.11.002**
11. Dooley, S., Won, S., Jahangirian. S., Ju. Y., Dryer. F., Wang. H., Oehlschlaeger, M.A., "The Combustion Kinetics of a Synthetic Paraffinic Jet Aviation Fuel and a Fundamentally Formulated, Experimentally Validated Surrogate Fuel", *Combustion and Flame*, **159**(10): **3014-3020**, 2012. DOI: **dx.doi.org/10.1016/j.combustflame.2012.04.010**.
12. Dooley. S., Dryer. F., Farouk. T.I., Ju. Y., Won. S., "Reduced Kinetic Models for the Combustion of Jet Propulsion Fuels", 51<sup>st</sup> Aerospace Sciences Meeting No AIAA 2013-0158, 2013. DOI: **10.2514/6.2013-158**.
13. Won. S., Veloo. P.S., Santner. J., Ju. Y., Dryer. F., "Comparative Evaluation of Global Combustion Properties of Alternative Jet Fuels", 51<sup>st</sup> Aerospace Sciences Meeting No AIAA 2013-0156, 2013. DOI: **10.2514/6.2013-156**.
14. Dryer. F., Ju. Y., Brezinsky. K., Santoro. R., Litzinger. T.A., Sung. C., "Science-based Design of Fuel-Flexible Chemical Propulsion/Energy", Final progress report, FA9550-07-7-0515, 2012.
15. Malewicki, T., Gudiyella. S., Brezinsky. K., "Experimental and Modeling Study on the Oxidation of Jet A and the n-dodecane/iso-octane/n-propylbenzene/1,3,5-trimethylbenzene Surrogate Fuel", *Combustion and Flame*, **160**(1): **17-30**, 2013. DOI: **10.1016/j.combustflame.2012.09.013**.
16. Honnet. S., Seshadri. K., Niemann. U., Peters. N., "A Surrogate Fuel for Kerosene", *Proceedings of the Combustion Institute*, **32**(1): **485-492**, 2009. DOI: **dx.doi.org/10.1016/j.proci.2008.06.218**.
17. Humer. S., Niemann. U., Seiser. R., Seshadri. K., Pucher. E., "Combustion of Jet Fuels and its Surrogates in Laminar Nonuniform Flows", *Proceedings of the European Combustion Meeting*, 2009.
18. Bruno. T.J., Smith. B.L., "Evaluation of the Physicochemical Authenticity of Aviation Kerosene Surrogate Mixtures. Part 1: Analysis of Volatility with the Advanced Distillation Curve", *Energy Fuels*, **24**(8): **4266-4276**, 2010. DOI: **10.1021/ef100496j**.
19. Bruno. T.J., Huber. M.L., "Evaluation of the Physicochemical Authenticity of Aviation Kerosene Surrogate Mixtures Part 2 Analysis and Prediction of Thermophysical Properties", *Energy Fuels*, **24**(8): **4277-4284**, 2010. DOI: **10.1021/ef1004978**.
20. Mueller. C.J., Cannella. W.J., Bruno. T.J., Bunting. B., Dettman. H.D., Franz. J.A., Huber. M.L., Natarajan. M., Pitz. W.J., Ratcliff. M.A., Wright. K., "Methodology for Formulating Diesel Surrogate Fuels with Accurate Compositional, Ignition-Quality, and Volatility Characteristics", *Energy Fuels*, **26**(6): **3284-3303**, 2012. DOI: **10.1021/ef300303e**.
21. Huber. M.L., Lemmon. E.W., Bruno. T.J., "Surrogate Mixture Models for the Thermophysical Properties of Aviation Fuel Jet-A", *Energy Fuels*, **24**(6): **3565-3571**, 2010. DOI: **10.1021/ef100208c**.
22. Huber. M.L., Smith. B.L., Ott. L.S., Bruno. T.J., "Surrogate Mixture Model for the Thermophysical Properties of Synthetic Aviation Fuel S-8: Explicit Application of the Advanced Distillation Curve", *Energy Fuels*, **22**(2): **1104-1114**, 2008. DOI: **10.1021/ef700562c**.
23. Violi. A., Yan. S., Eddings. E.G., Granata. S., Faravaelli. T., Ranzi. E., "Experimental Formulation and Kinetic Model for JP-8 Surrogate Mixtures", *Combustion Science and Technology*, **171**(11): **399-417**, 2002. DOI: **10.1080/00102200215080**.
24. Lai, M., Zhou, B., Wong, V.W., Cheng, W.K., Benedek, K.P., "A Parametric Study of Coal-Water Slurry Injection and Combustion in a Rapid Compression Machine," *ASME Energy-Sources Technology Conferences and Exhibition*, Dallas, TX, ASME paper 87 ICE-9, 1987.
25. Lu. P., Han. J., Lai. M., Henein. N.A., Bryzik. W., "Combustion Visualization of DI Diesel Spray Combustion inside a Small-Bore Cylinder under different EGR and Swirl Ratios", *SAE Technical Paper*, **2001-01-2005**, 2001. DOI: **10.4271/2001-01-2005**.
26. Lu, P., Xie, X., Lai, M., "Spectral Analysis and Chemiluminescence Imaging of Hydrogen Addition to HSDI Diesel Combustion Under Conventional and Low-Temperature Conditions," *SAE Technical Paper*, **2004-01-2919**, 2004. DOI: **10.4271/2004-01-2919**.
27. Matsumoto, A., Zheng, Y., Xie, X., Lai, M., Moore. W., "Characterization of Multi-hole Spray and Mixing of Ethanol and Gasoline Fuels under DI Engine Conditions", *SAE Technical Paper*, **2010-01-2151**, 2010. DOI: **10.4271/2010-01-2151**.
28. Matsumoto, A., Moore, W., Lai, M., Zheng, Y., Foster. M., Xie. X., Yen. D., Confer. K., Hopkins. E., "Spray Characterization of Ethanol Gasoline Blends and Comparison to a CFD Model for a Gasoline Direct Injector," *SAE Int. J. Engines*, **3**(1): **402-425**, 2010, DOI: **10.4271/2010-01-0601**.
29. Matsumoto, A., "Spray Characterization of Flex-fuel Gasoline DI Injectors and Spray Interaction with Charge Motion in a Variable Valve Actuation Engine", PH.D dissertation, Wayne State University, Detroit, 2012.
30. American Society for Testing and Materials, "Standard Test Method for Determination of Ignition Delay and



- Derived Cetane Number (DCN) of Diesel Fuel Oils by Combustion in a Constant Volume Chamber". **ASTM D6890-10a**, Rev. Aug 2010.
31. Zheng, Z., Badawy, T., Henein, N.A., Sattler, E., "Investigation of Physical and Chemical Delay Periods of Different Fuels in the Ignition Quality Tester", *J. Eng. Gas Turbines Power* **135**(6), **061501**, 2013. DOI: **10.1115/1.4023607**.
  32. Zheng, Z., Badawy, T., Henein, N.A., Sattler, E., Johnson, N., "Effect of Cetane Improver on Autoignition Characteristics of Low Cetane Sasol IPK Using Ignition Quality Tester", ASME ICEF Conference, **ICEF2013-19061**, 2013.
  33. Henein, N. A., Bolt, J. A., "Correlation of Air Charge Temperature and Ignition Delay for Several Fuels in a Diesel Engine". SAE Technical Paper, **690252**, 1969. DOI: **10.4271/690252**.
  34. Henein, N. A., Elias, N. Y., "A Modified Cetane Scale for Low Ignition Quality Fuels". SAE Technical Paper, **780640**, 1978. DOI: **10.4271/780640**.
  35. Ryan, T. W., Callahan, T. J., "Engine and Constant Volume Bomb Studies of Diesel ignition and Combustion". SAE Technical Paper, **881626**, 1988. DOI: **10.4271/881626**.
  36. Lin, C. S. and Foster, D. E., "An Analysis of Ignition Delay, Heat Transfer and Combustion During Dynamic Load Changes in a Diesel Engine". SAE Technical Paper **892054**, 1989. DOI: **10.4271/892054**.
  37. Aradi, A. A., Ryan, T. W., "Cetane Effect on Diesel Ignition Delay Times Measured in a Constant Volume Combustion Apparatus". SAE Technical Paper, **952352**, 1995. DOI: **10.4271/952352**.
  38. Bogin, G., Osecky, E., Ratcliff, M. A., Luecke, J., He, X., Zigler, B., Dean, A. M., "Ignition Quality Tester (IQT) Investigation of the Negative Temperature Coefficient Region of Alkane Autoignition", *Energy and Fuels*, **27**(3): **1632-1642**, 2013. DOI: **10.1021/ef301738b**.
  39. Bogin, G., Dean, A. M., Ratcliff, M. A., Luecke, J., Zigler, B., "Expanding the Experimental Capabilities of the Ignition Quality Tester for Autoigniting Fuels", SAE Technical Paper, **2010-01-0741**, 2010. DOI: **10.4271/2010-01-0741**.
  40. American Society for Testing and Materials, "Standard Test Method for Distillation of Petroleum Products at Atmospheric Pressure", **ASTM D86-12**, Rev. 2012.
  41. Aspen HYSYS V7.3, Computer software, Aspen Technology, Inc, Massachusetts, USA, 1994-2013.
  42. Shrestha, A., Zheng, Z., Badawy, T., Henein, N.A., "Development of JP-8 Surrogates and their Validation using Ignition Quality Tester", SAE J. Fuel & Lube, 13JFL-0027 (submitted and under review), 2013.
  43. Mueller, C., "The Quantification of Mixture Stoichiometry When Fuel Molecules Contain Oxidizer Elements or Oxidizer Molecules Contain Fuel Elements", SAE Technical Paper, **2005-01-3705**, 2005. DOI: **10.4271/2005-01-3705**.
  44. Holley, A.T., You, X.Q., Dames, E., Wang, H., Egolfopoulos, F.N., "Sensitivity of Propagation and Extinction of Large Hydrocarbon Flames to Fuel Diffusion", *Proceedings of the Combustion Institute*, **32**(1): **1157-1163**, 2009. DOI: **dx.doi.org/10.1016/j.proci.2008.05.067**
  45. Riesmeir, E., Honnet, S., Peters, N., "Flamelet Modeling of Pollutant Formation in a Gas Turbine Combustion Chamber Using Detailed Chemistry for a Kerosene Model Fuel", *J. Eng. Gas Turbine Power*, **126**(4): **899-905**, 2004. DOI: **10.1115/1.1787507**.
  46. Violi, A., Martz, J., Elvati, P., Kim, D., "Combustion Behavior and Fuel Economy of Modern Heavy-Duty Diesel Engine Using JP-8 and Alternative Fuels", presented at ARC conference, University of Michigan, USA, May 21-22, 2012.
  47. Gill, S.S., Tsolakis, A., Dearn, K.D., Rodríguez-Fernández, J., "Combustion Characteristics and Emissions of Fischer-Tropsch Diesel Fuels in IC Engines", *Progress in Energy and Combustion Science*, **34**(4): **503-523**, 2011. DOI: **dx.doi.org/10.1016/j.pecs.2010.09.001**.
  48. NIST Chemistry Book, NIST Standard Reference Database Number 69, <http://webbook.nist.gov/chemistry/>, July 2013.
  49. Smith, E. B., "Basic Chemical Thermodynamics". Clarendon Press, Oxford, 1993.
  50. Pickett, L., Hoogterp, L., "Fundamental Spray and Combustion Measurements of JP-8 at Diesel Conditions". SAE Technical Paper, **2008-01-1083**, 2008. DOI: **10.4271/2008-01-1083**.
  51. Henein, N. A., Bolt, J. A., "Correlation of Air Charge Temperature and Ignition Delay for Several Fuels in a Diesel Engine". SAE Technical Paper, **690252**, 1969. DOI: **10.4271/690252**.
  52. He, X., Donovan, M.T., Zigler, B.T., Palmer, T.R., Walton, S.M., Wooldridge, M.S., Atreya, A., "An experimental and modeling study of iso-octane ignition delay times under homogeneous charge compression ignition conditions", *Combustion and Flame*, **142**(3): **266-275**, 2005. DOI: **10.1016/j.combustflame.2005.02.014**.
  53. Frauwallner, M., López-Linares, F., Lara-Romero, J., Scott, C.E., Ali, V., Hernández, E., Pereira-Almao, P., "Toluene Hydrogenation at Low Temperature using a Molybdenum Carbide Catalyst", *Applied Catalysis A: General*, **394**(1): **62-70**, 2011. DOI: **dx.doi.org/10.1016/j.apcata.2010.12.024**
  54. Henein, N., "Cetane Scale: Function, Problems and Possible Solutions," SAE Technical Paper, **870584**, 1987, DOI: **10.4271/870584**.
  55. Siebers, D., "Ignition Delay Characteristics of Alternative Diesel Fuels: Implications on Cetane Number," SAE Technical Paper, **852102**, 1985, DOI: **10.4271/852102**.

## Contact Information

Ziliang Zheng

Research Assistant

Wayne State University, Detroit, MI

zhengziliang@gmail.com

Po-I Lee

Research Assistant

Wayne State University, Detroit, MI

bb9304@wayne.edu

Dr. Naeim Henein

Professor

Wayne State University, Detroit, MI

henein@eng.wayne.edu

## **Acknowledgments**

This research was sponsored by the US Army RDECOM-TARDEC and Automotive Research Center (ARC): a Center of Excellence in Simulation and Modeling sponsored by the US Army RDECOM-TARDEC, led by the University of Michigan. Our special thanks go to Patsy Muzzell and Peter Schihl of TARDEC, as well as Kapila Wadumesthrige of Next Energy and Dr. Xingbin Xie of Wayne State University for their technical support. Also, we would like to thank Dr. Bradley Zigler of the National Renewable Energy Laboratory, Dr. Frederick Dryer of Princeton University for their technical support and Wayne State University Center for Automotive Research (CAR) members for their help in conducting this research.

**Definitions/Abbreviations****NL**

Needlelift

**ARHR** Apparent Rate of Heat Release**NTC**

Negative Temperature Coefficient

**CI** Compression Ignition**PFR**

Pressurized Flow Reactor

**CN** Cetane Number**POI**

Point of Inflection

**DAQ** Data Acquisition**RCM**

Rapid Compression Machine

**DCN** Derived Cetane Number**RHR**

Same as ARHR

**Ea** Apparent Activation Energy**R<sub>u</sub>**

Universal Gas Constant

**FFT** Fast Fourier Transform**SOI**

Start of Injection

**FPS** Frame Per Second**SwRI**

Southwest Research institute

**IC** Internal Combustion**TDC**

Top Dead Center

**ID** Ignition Delay**TSI**

Threshold Sooting Index

**IQT** Ignition Quality Tester**JP-8** Jet Propellant 8**LHV** Lower Heating Value**MW** Molecular Weight**NI** National Instrument




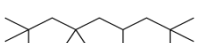

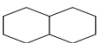

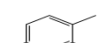


## Appendix

Table A1. Properties of JP-8

	Test Method	JP-8
Derived Cetane Number	ASTM D6890	49.24
Density (g/ml)	ASTM D1298	0.802
Hydrogen/Carbon Ratio	ASTM D5291	1.93
Low Heating Value (MJ/kg)	ASTM D3338	43.2
Molecular Weight (g/mol)	CORE*	161
Threshold Sooting Index	ASTM D1322	22.96
Viscosity @ 40°C	ASTM D445	1.368
n-alkanes (%vol)	ASTM D2425	9.2
Iso-alkanes (%vol)	ASTM D2425	29.8
Cyclo-alkane (%vol)	ASTM D2425	44.5
Aromatics (%vol)	ASTM D2425	12.6
Other (%vol)	ASTM D2425	3.9

\*CORE MW is the test method for the determination of average molecular weight followed by Core Laboratories, Deer Park, Texas. The repeatability of the method was reported to be very accurate with percent standard deviation of 1.

Table A2. Properties of Pure Component

Compound Name	Molecular Structure	Molecular Formula	CAS Number
n-hexadecane		C <sub>16</sub> H <sub>34</sub>	554-76-3
n-dodecane		C <sub>12</sub> H <sub>26</sub>	112-40-3
n-decane		C <sub>10</sub> H <sub>22</sub>	124-18-5
2,2,4,4,6,8,8-heptamethylnonane (iso-cetane)		C <sub>16</sub> H <sub>34</sub>	4390-04-9
2,2,4-trimethylpentane (iso-octane)		C <sub>8</sub> H <sub>18</sub>	540-84-1
decahydronaphthalene (decalin)		C <sub>10</sub> H <sub>18</sub>	91-17-8
methylcyclohexane		C <sub>7</sub> H <sub>14</sub>	108-87-2
1,2,4-trimethylbenzene		C <sub>9</sub> H <sub>12</sub>	95-63-6
m-xylene		C <sub>8</sub> H <sub>10</sub>	108-38-3
toluene		C <sub>7</sub> H <sub>8</sub>	108-88-3